GeoScienceWorld
Lithosphere
Volume 2022, Article ID 8798300, 14 pages
https://doi.org/10.2113/2022/8798300

Lithosphere

*Research Article*

# Study on Stability and Control of Pre-excavated Withdrawal Channel under Mining Influence

**Hanrui Zhang, Changyou Liu, Xin Yu, Kun Zhang, and Huaidong Liu**

*School of Mines, China University of Mining and Technology, Xuzhou 221116, China*

Correspondence should be addressed to Changyou Liu; cyliu20222022@163.com

Received 26 June 2022; Revised 30 October 2022; Accepted 12 November 2022; Published 1 December 2022

Academic Editor: Qian Liu



Pre-excavated withdrawal channel (PWC) is an effective means to shorten the withdrawal time of fully mechanized working face and improve the efficiency, safety, and reliability during the withdrawal. However, the key to the success of the withdrawal method is the influence of mining on the stability of PWC, taking the $III32_{upper}1$ working face of Zhuzhuang Coal Mine as the engineering background. By theoretical analysis and numerical simulation, the deformation of the PWC is analyzed and the mechanical model of the influence of the instability of the main roof fracture on the PWC is established. And the effect of the fracture and rotation of the main roof on the PWC is analyzed. The result shows that the instability of the coal pillar leads to the fracture and rotary deformation of the main roof as the width of the coal pillar gradually decreases, which further aggravates the deformation of the PWC and the degree of ground pressure behavior. Based on the influence of mining on the PWC, a control method is proposed. This method uses hydraulic fracturing technology to weaken the mining stress and prevent the fracture of the main roof above the PWC. The control effect of hydraulic fracturing on PWC is analyzed through the establishment of numerical calculation model. The result of engineering practice demonstrates that the mining stress is significantly reduced, and the deformation of surrounding rock in the PWC is effectively controlled after hydraulic fracturing.

## 1. Introduction

The safe and rapid withdrawal is an important part in the production and is also an important content in the terminal operation of working face [1]. There are many ways of withdrawal of working face. Among them, PWC is one of the most common ways to achieve rapid withdrawal of equipment [2, 3]. However, the stability of the PWC is the prerequisite for the safe and rapid withdrawal [4]. Since the PWC is affected by the front abutment pressure of the working face and the stability of the main roof, it is necessary to take technical measures in advance to ensure safe and rapid withdrawal [5, 6].

Many scholars have done a series of research on guaranteeing the stability of PWC. Wang et al. explored the stress evolution and cumulative damage mechanism of coal pillar during mining disturbance [7]. Lv established a mechanical model of unmined coal pillar and revealed the dynamic characteristics of coal pillar [8]. He et al. and He and Li studied the damage features and optimal spacing of double withdrawal channel [9, 10]. Gu et al. analyzed the impact factors of the stability of the PWC before different ground pressure adjustment and studied the stress distribution of coal pillar at the end mining stage [11, 12]. Liu et al. and Lv et al. investigated the stress and deformation characteristics of surrounding rock of PWC under different mining conditions [13, 14]. Wang et al. found that the last weighting and the fracture position of the main roof are the key affecting the stability of the PWC [15]. Li et al. elaborate on the reasons for the asymmetric disruption of the PWC [16]. Feng et al. examined the relationship between the width of the coal pillar and the stability of the PWC by numerical simulation [17].

In view of the severe deformation of the PWC in the end mining stage, Ma et al. and Guo and Hong put forward the idea of controlling the stability of PWC by blasting roof cutting [18, 19]. He et al. proposed a zoning control strategy with high pressure water jet and asymmetric high strength cable beam network and three hole anchor cable groups and roof grouting as the core [20]. Zhang et al. presented a

fixed-length roof cutting technology with vertical hydraulic fracture [21]. Qin et al. and Wang et al. introduced sectional excavation technology and combined support technology of anchor and bolt [22, 23]. Kang et al. analyzed the loading mechanisms of predriven longwall recovery rooms subjected to large abutment pressures and designed a reasonable support plan [24]. Feng and Wu put forward the support method of anchor cable and grouting Marisan [25]. Yang and Zhu raised the stoping and pressure releasing technology of the terminal mining section based on controlling the fracture position of main roof [26].

It can be seen that the existing related research mainly protect the stability of the PWC by strengthening support or forced caving, which plays a positive role in rapid and safe withdrawal. But it still needs a great deal of work to weaken the mining stress to guarantee the stability of the PWC. Therefore, this paper investigates the deformation of the PWC under the influence of mining and stability of the main roof. Based on this, a hydraulic fracturing pressure releasing control method is proposed. By analyzing the control effect and time-space relationship of this method, it provides a theoretical basis for the hydraulic fracturing control of PWC.

## 2. Surrounding Rock Deformation of Pre-excavated Withdrawal Channel under Mining Influence

With the decrease of the distance between the working face and the PWC, the width of the coal pillar gradually decreases. When the influence range of advance abutment pressure is greater than the width of coal pillar, the mining will affect the stability of PWC. Therefore, the UDEC numerical calculation model is used to analyze the surrounding rock deformation of PWC.

*2.1. Engineering Geological Condition.* The study site was the $III32_{upper}1$ working face in the Zhuzhuang Coal Mine located at Anhui Province, China. The buried depth of the working face is 220 m~250 m. It was approximately 670 m long and 172 m wide. The width and height of the PWC are 4.4 m and 2.4 m. Layout of working face and columnar diagram of strata are shown in Figure 1. The PWC is perpendicular to the headgate and tailgate and is arranged in the position of the terminal line, as shown in Figure 2.

*2.2. Establishment of Numerical Model.* Based on the geological conditions of $III32_{upper}1$ working face in Zhuzhuang Coal Mine, the UDEC numerical simulation model is established, as shown in Figure 3. The length of the model is 200 m and the height is 41.3 m. The depth of the coal seam is about 240 m, and the PWC is excavated in advance in the model. The PWC is 4.4 m wide and 2.4 m high. The bottom boundary of the model is fixed in the vertical direction; the left and right boundaries limit the horizontal displacement. The vertical stress of 5.1 MPa is applied to the upper boundary to simulate the overburden load. The physical and mechanical parameters of coal and rock mass are shown in Table 1.

*2.3. Analysis of Surrounding Rock Deformation of Pre-excavated Withdrawal Channel.* The stress distribution of the surrounding rock of the PWC is shown in Figure 4. It can be seen from the figure that the stress disturbance range is small when the working face is far from the PWC, and the peak stress of the coal pillar on the right side of the PWC is 10.00 MPa. When the width of the coal pillar in the working face is 25 m, the stress of the coal pillar increases obviously, which indicates that the PWC has entered the influence range of the advanced abutment pressure of the working face, and the peak stress of the right coal pillar increases to 12.56 MPa. When the distance between the working face and the PWC is 15 m, the peak stress of the right coal pillar reaches the highest, and the peak value is 16.85 MPa. When the width of the coal pillar is 10 m, the coal pillar is destroyed and gradually loses its bearing capacity, and the peak stress gradually decreases. When the width is 5 m, the peak stress has been reduced to 5.67 MPa.

Figure 5 illustrates the deformation of surrounding rock of PWC. The result shows that the advance abutment pressure has little effect on the stability of the PWC when the working face is more than 25 m away from the PWC. At the moment, the deformation is small and the surrounding rock is relatively stable. With the advance of working face, the front abutment pressure of working face and side abutment pressure of roadway are superposed. The influence of mining on the stability of the PWC increases, and the convergence of the roof and floor and the two ribs increases significantly. The maximum deformation of the roof, floor, rib of coal pillar, and rib of solid coal of the PWC is 469.7 mm, 1074.1 mm, 753.4 mm, and 399.9 mm, respectively. When the working face is 5 m away from the PWC, the deformation speed of surrounding rock reaches the maximum because the unmined coal pillar loses its bearing capacity. The deformation speed is 145.3 mm/d, 311.2 mm/d, 179.9 mm/d, and 76.7 mm/d, respectively.

## 3. Influence of Stability of Main Roof Structure on Pre-excavated Withdrawal Channel

*3.1. Dynamic Changes of Fracture Instability of Main Roof above Pre-excavated Withdrawal Channel.* In the process of working face advancing, the main roof will experience periodic fracture and instability process. Considering the most dangerous situation, that is, the fracture line of the main roof is located above the PWC [27]. As shown in Figure 6, in this case, the main roof will undergo the following three changes from stability to instability.

When the coal pillar between the working face and the PWC is wide, the main roof is not broken due to the support of the coal pillar and the hydraulic powered support. At this time, the main roof is in a cantilever beam state, as shown in Figure 6(a).

As the working face gradually approaches the PWC, the main roof fractures above the PWC when the hanging length of rock block A reaches the fracture limit. Rock block A and rock block B undergo rotation and extrusion. At this time, due to the large free space between the main roof and the

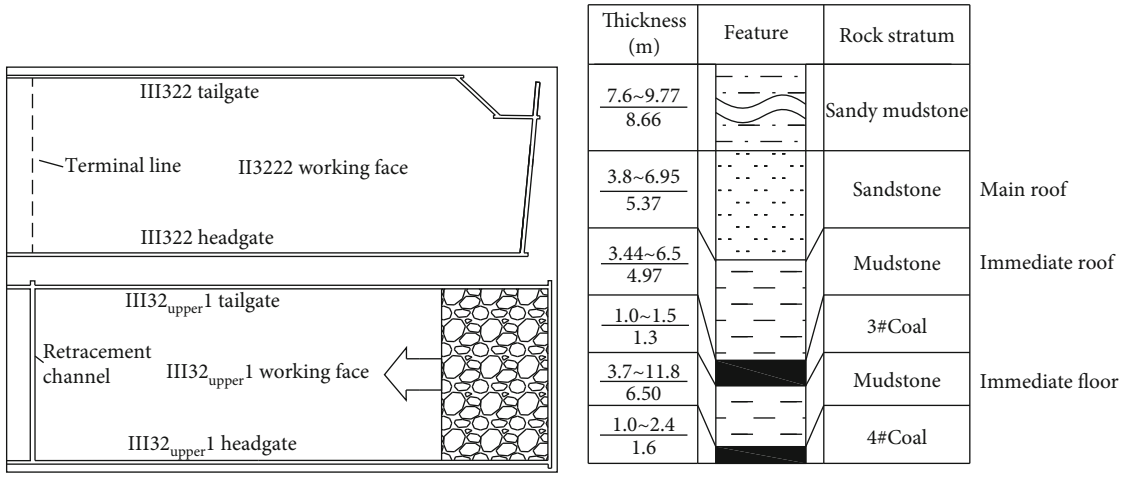


Figure 1: Layout of working face and columnar diagram of strata.


Figure 2: The site pictures of the PWC.

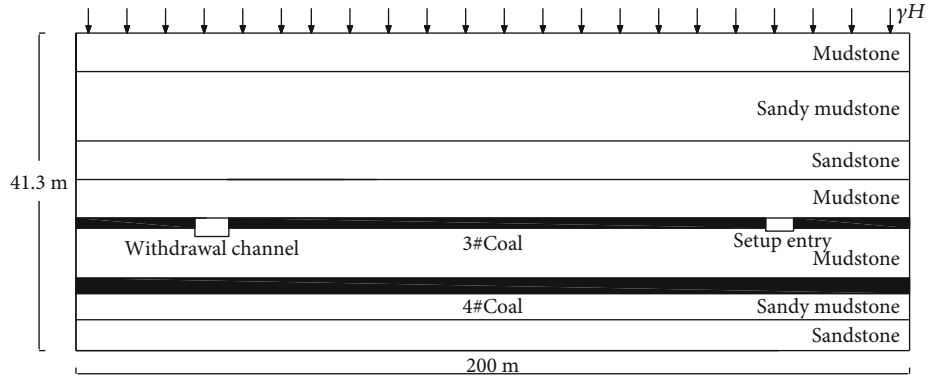


Figure 3: Numerical model simplified diagram.

gangue in the gob, the rock block A has not touched the gangue, as shown in Figure 6(b).

With the continuous advancement of the working face, rock block A continues to rotate and rock block B continues to rotate reversely with rock block A. The rotation angle of rock block A gradually increases, and the contact area with rock block B gradually increases. When rock block A rotates to touch the gangue, the load of roof structure is mainly supported by gangue in gob, as shown in Figure 6(c).

From the dynamic changes of the fracture and instability of the main roof, it can be seen that the coal pillar is broken and unstable under the influence of mining due to the decrease of width of the coal pillar. The fracture and instability of the main roof is caused by the sudden disappearance of

Table 1: Physical and mechanical parameters of coal and rock mass.

| Strata | Density (kg/m$^3$) | Bulk modulus (GPa) | Shear modulus (GPa) | Force of cohesion (MPa) | Angle of internal friction (°) | Tensile strength (Mpa) |
|---|---|---|---|---|---|---|
| Mudstone | 2300 | 5 | 3 | 1.5 | 22 | 2.3 |
| Sandy mudstone | 2260 | 6.1 | 3.9 | 2.2 | 23 | 4.2 |
| Sandstone | 2200 | 7 | 5 | 3 | 25 | 6.5 |
| Mudstone | 2300 | 4.5 | 2.8 | 1.5 | 22 | 2.3 |
| 3#Coal | 1440 | 2 | 1.5 | 1.25 | 20 | 2 |
| Mudstone | 2300 | 5 | 3 | 2.07 | 22 | 2.5 |
| 4#Coal | 1440 | 2 | 1.5 | 1.25 | 20 | 2 |
| Sandy mudstone | 2260 | 6.1 | 3.9 | 2.2 | 23 | 4.2 |
| Sandstone | 2200 | 7 | 5 | 3 | 25 | 6.5 |

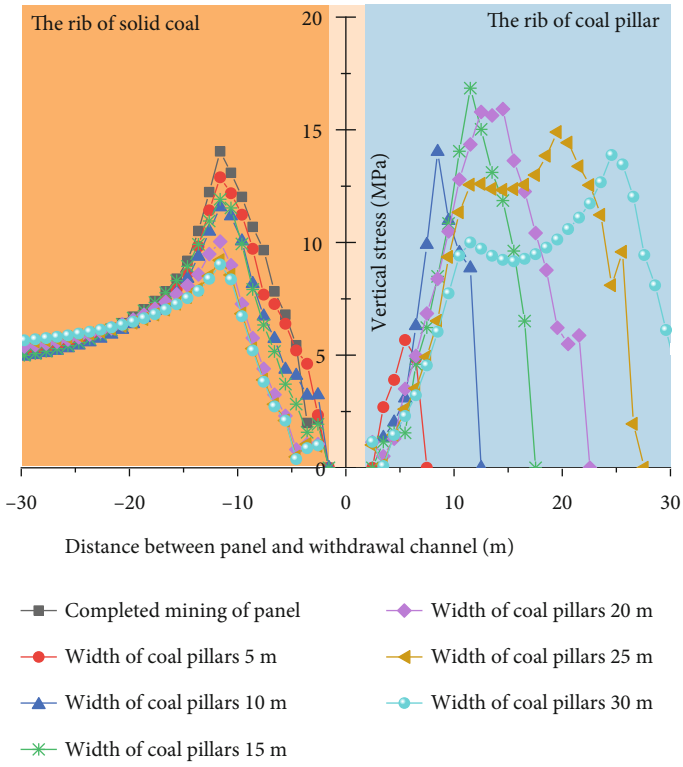


Figure 4: Stress distribution characteristics of coal pillar on both sides of PWC.

the effective support of the coal pillar to the main roof. At the same time, the fracture and rotation of the main roof will further aggravate the deformation of the PWC and the degree of ground pressure behavior.

*3.2. Mechanical Analysis of Stability of Main Roof Structure above Pre-excavated Withdrawal Channel.* According to the analysis of the fracture characteristics of the main roof, rock block A is the key to ensure the stability of the PWC. Therefore, the structural mechanic model of rock block A is established to analyze the condition for the rotary deformation and instability of rock block A, and the condition that the support resistance of the hydraulic powered support in the working face needs to meet when the rotary instability occurs.

In the mechanical model of Figure 7, $l$ is the length of rock block A, m; $q$ is the weight per unit length of rock block A and overlying strata, MN/m; $T$ is the horizontal thrust of rock block A, and $\alpha$ is the rotation angle of rock block A, °; $h$ is the thickness of the main roof, m; $a$ is the length of the contact surface between rock blocks, m; $F_g$ is the supporting reaction force of gob, MN; $F_z$ is the support resistance of the working face hydraulic powered support, MN; $F_c$ is the support resistance of the chock hydraulic support, MN; $W$ and $L_K$ are the width of the PWC and the control distance of the working face support, m; the

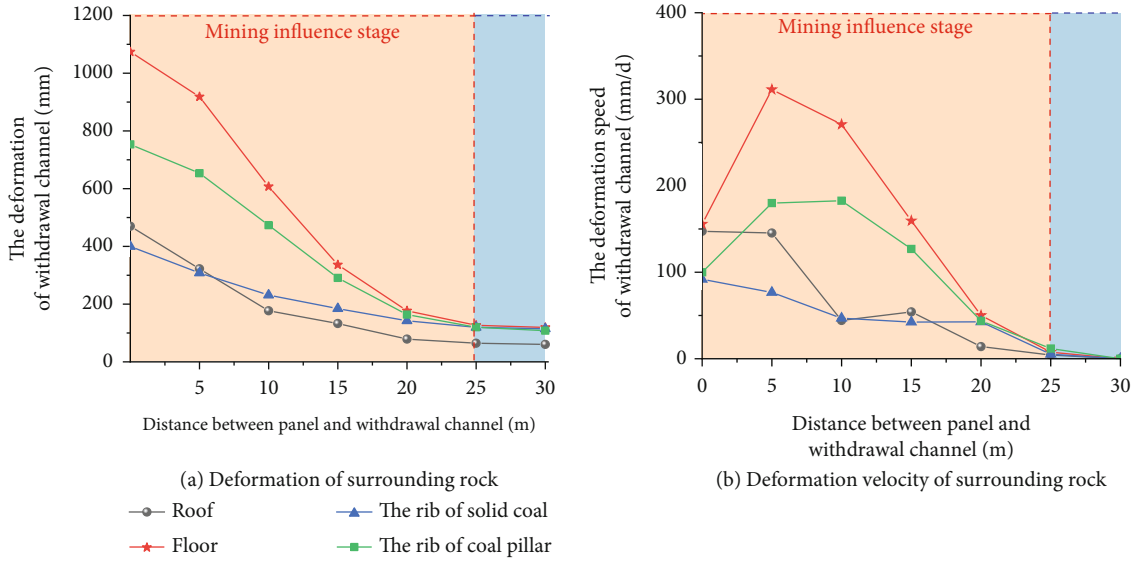


Figure 5: Deformation of surrounding rock of PWC.

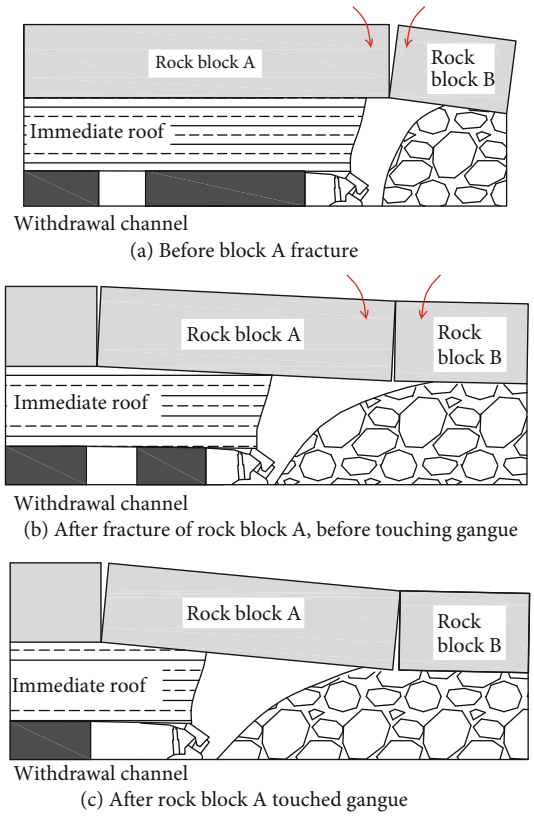


Figure 6: Dynamic process of main roof rotation.

resultant force of $F_z$ acts at $L_K/2$; and the resultant force of $F_c$ acts at $W/3$.

To prevent rock block A from rotary instability, the following condition must be met:

$$\frac{T}{a} \leq \eta\sigma_c, \tag{1}$$

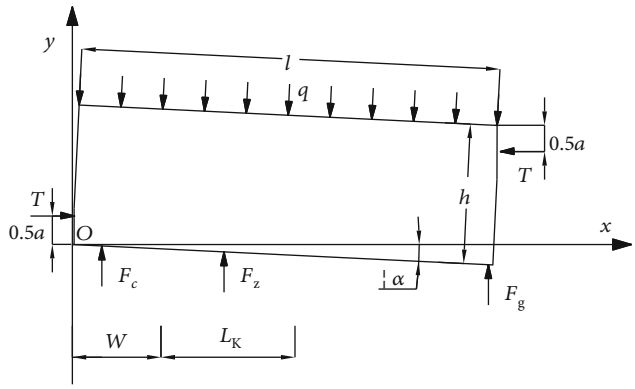


Figure 7: Force analysis of rock block A.

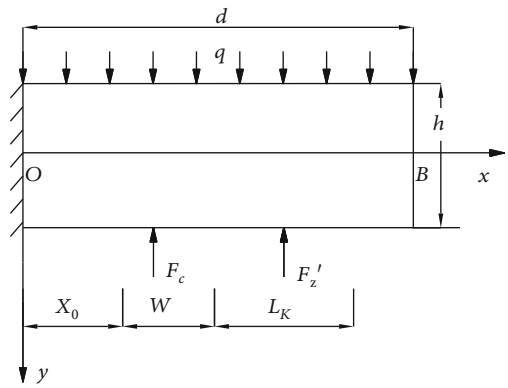


Figure 8: Force analysis of main roof after artificial roof cutting.

where $T/a$ is the average extrusion stress on the contact surface; $\eta$ is the coefficient taken for special stress of rock block at the corner, 0.3; and $\sigma_c$ is the compressive strength of rock block, MPa.

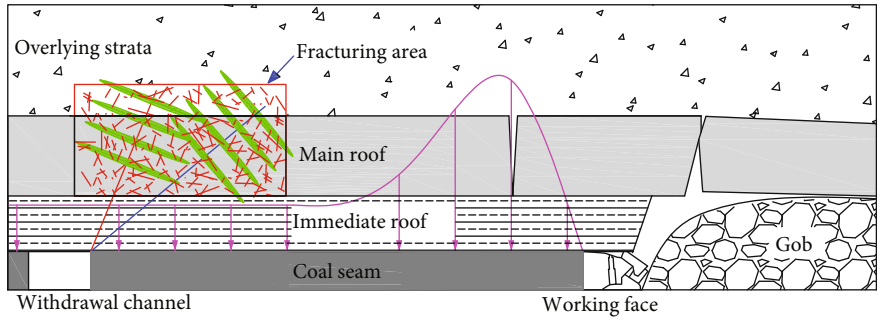


Figure 9: Schematic diagram of hydraulic fracturing control of PWC.

Establish the moment equilibrium equation at point O:

$$\frac{1}{2}ql^2 = \frac{F_c W}{3} + F_z\left(W + \frac{L_K}{2}\right) + F_g l + T(h - l\sin\alpha - a). \tag{2}$$

Among them, the contact surface length $a$ between rock blocks can be expressed as

$$a = \frac{1}{2}(h - l\sin\alpha). \tag{3}$$

The supporting reaction force $F_g$ of gangue in gob can be expressed as [28]

$$F_g = \frac{\Delta}{h_1 K_p}E_i, \tag{4}$$

where $\Delta$ is the compression deformation of gangue, m; $h_1$ is the thickness of immediate roof, m; $K_p$ is the bulk increase coefficient of gangue; and $E_i$ is the elastic modulus of gangue, MPa.

The horizontal thrust $T$ can be obtained using Equations (2)–(4) as presented:

$$T = \frac{ql^2 - (2/3)F_c W - F_z(2W + L_K) - \left(2\left(\Delta/h_1 K_p\right)\right)E_i l}{h - l\sin\alpha}. \tag{5}$$

Combining Equations (1) and (5), the condition that the support resistance $F_z$ of the working face hydraulic powered support needs to meet can be expressed as

$$F_z \geq \frac{\left[\left(\left(ql^2/2\right) - (1/3)\right)\left(F_c W - \left(\Delta/h_1 K_p\right)\right)\right)\left(\left(E_i l - (1/4)\right)\left(\eta\sigma_c(h - l\sin\alpha)^2\right)\right)\right]}{(W + (L_k/2))}. \tag{6}$$

It can be seen from Equation (6) that the support resistance $F_z$ of the working face hydraulic powered support is proportional to the rotation angle $\alpha$ of rock block A. With the decrease of the width of unmined pillars in the working face, the rotation angle of rock block A gradually increases, and the support resistance of the hydraulic support in the working face also increases. When rock block A undergoes rotary deformation and instability, the support resistance of the hydraulic powered support needs to meet the conditions in Equation (6).

*3.3. Stability Analysis of Main Roof under Artificial Roof Cutting Condition.* Based on the influence of the natural fracture and instability of the main roof, the PWC can be put under the stable cantilever rock beam by artificial roof cutting in advance, so as to avoid the influence of the natural fracture and rotary deformation of the main roof on the PWC and improve the stability of the surrounding rock of the roadway.

Through artificial roof cutting, the fracture line of the main roof is controlled behind the working face. At this time, the main roof above the PWC is a cantilever beam structure, and the mechanical model is established for analysis, as shown in Figure 8. Where $q$ is the load of overlying strata; $h$ is the thickness of the main roof; $d$ is the distance from the plastic zone of coal rib to the fracture position of the roof; and $X_0$ is the width of plastic zone of the coal rib.

The force of main roof includes the load of overlying strata $q$, the support resistance $F_c$ of the chock hydraulic support, and the rating support resistance $F_z'$ of the working face hydraulic powered support. The deflection deformation caused by each force is calculated separately, and the final deflection deformation of the main roof can be obtained by the sum of each deflection deformation.

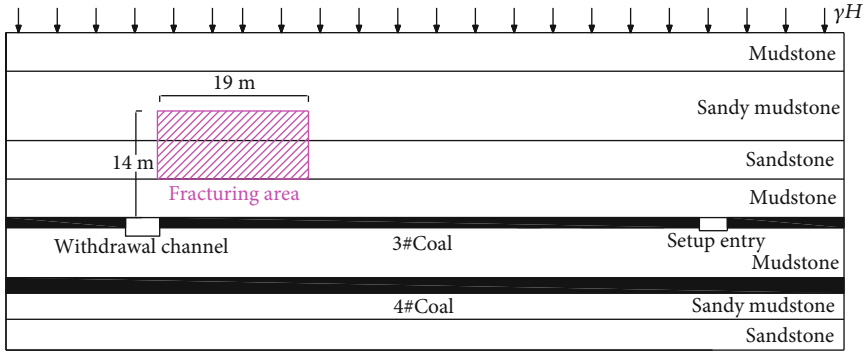


Figure 10: UDEC numerical calculation model diagram.

Table 2: Mechanical parameters of sandstone with different damage levels.

| Scheme number | Damage variable | Bulk modulus (GPa) | Shear modulus (GPa) | Force of cohesion (MPa) | Angle of internal friction (°) |
|---|---|---|---|---|---|
| 1 | $D = 0$ | 7 | 5 | 3 | 25.00 |
| 2 | $D = 0.1$ | 6.45 | 4.52 | 2.79 | 23.37 |
| 3 | $D = 0.2$ | 5.88 | 4.04 | 2.63 | 21.24 |
| 4 | $D = 0.3$ | 4.96 | 3.48 | 2.46 | 20.03 |
| 5 | $D = 0.4$ | 4.15 | 2.88 | 2.25 | 18.24 |
| 6 | $D = 0.5$ | 3.43 | 2.47 | 2.07 | 16.55 |

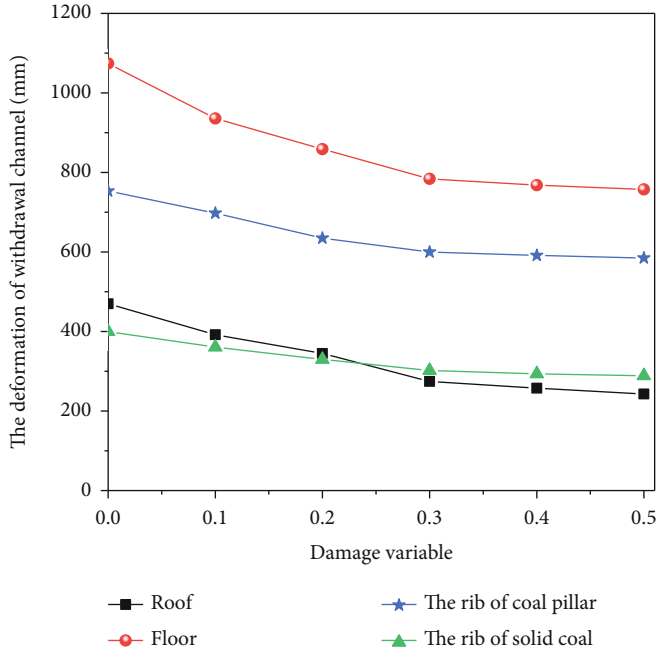


Figure 11: Influence of fracturing degree on surrounding rock deformation of PWC.

According to the deflection equation of cantilever beam, the deflection of cantilever beam under the action of load $q$ at point B can be expressed as

$$(w_B)_q = \frac{qd^4}{8E_mI}, \tag{7}$$

where $E_m$ is the main roof elastic modulus and $I$ is the inertial moment of the main roof section.

In order to simplify the calculation process, according to Saint-Venant's principle, the deflection of cantilever beam under the support resistance $F_z'$ of the hydraulic powered support can be expressed as

$$(w_B)_{F_z} = -\frac{F_z'd^3}{3E_mI} + \frac{F_z'(d - X_0 - W - (L_K/2))d^2}{2E_mI}. \tag{8}$$

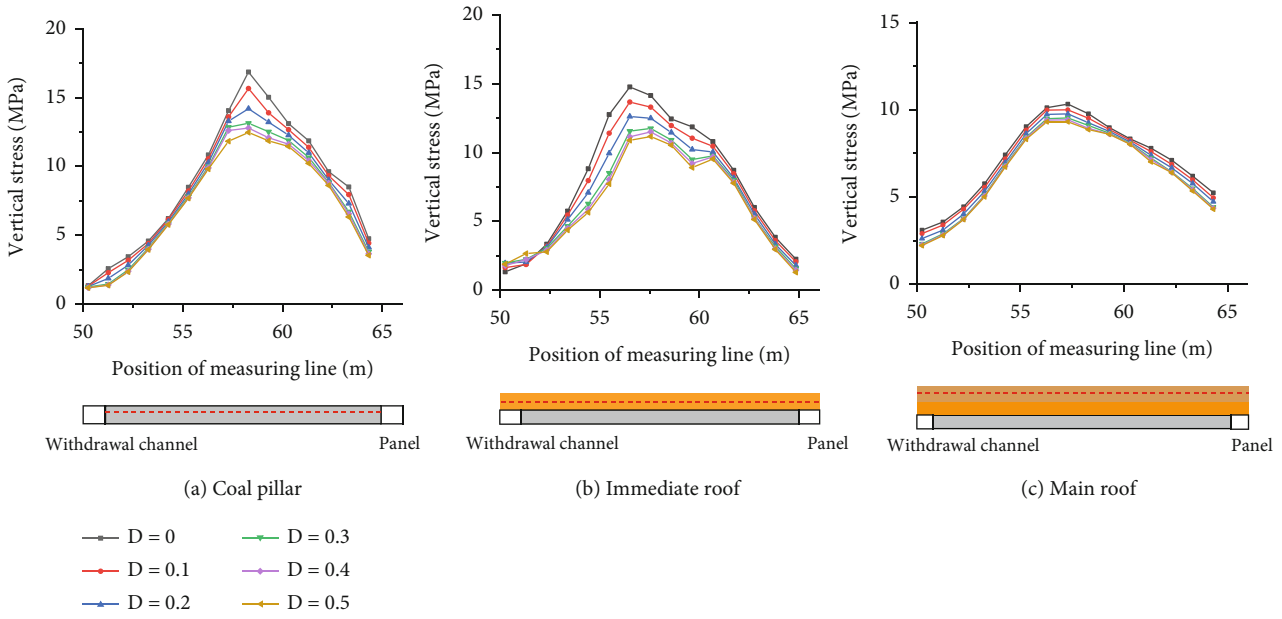


Figure 12: The influence law of fracturing degree on the stress distribution of surrounding rock.

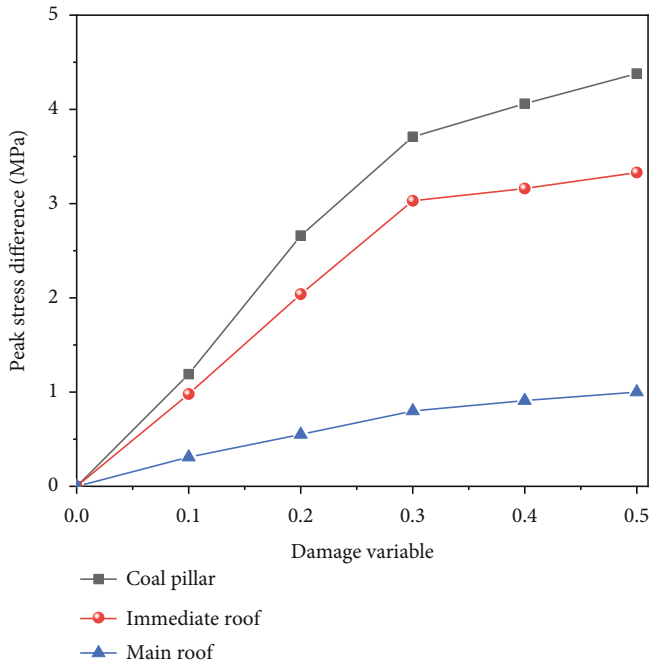


Figure 13: Variation rule of peak stress difference under different damage variables.

Similarly, the deflection under the support resistance $F_c$ can be expressed as

$$(w_B)_{F_c} = -\frac{F_c d^3}{3E_m I} + \frac{F_c(d - X_0 - (W/3))d^2}{2E_m I}. \quad (9)$$

The final deflection deformation of the main roof can be obtained with the summation of Equations (7)–(9) as presented:

$$w_B = \frac{qd^4}{8E_m I} - \frac{\left(F_z' + F_c\right)d^3}{3E_m I} + \frac{F_z'(d - X_0 - W - (L_K/2))d^2 + F_c(d - X_0 - (W/3))d^2}{2E_m I}. \quad (10)$$

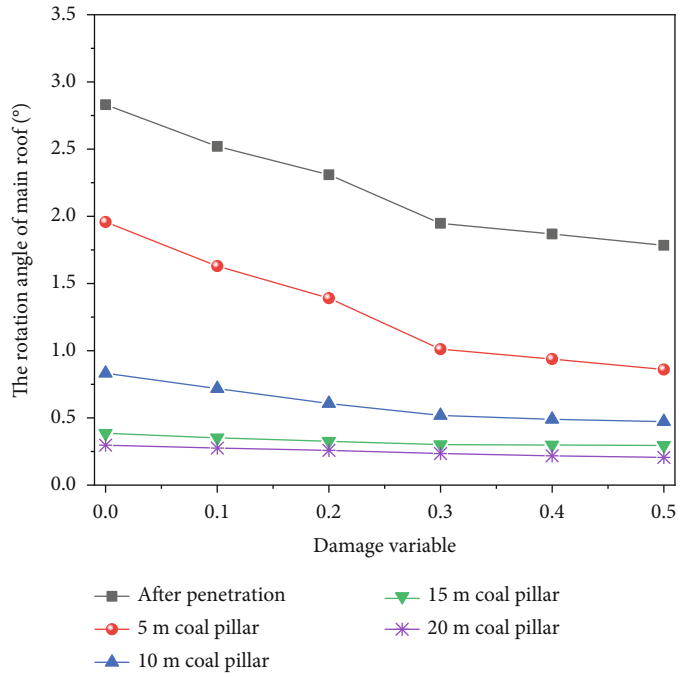


Figure 14: Influence law of fracturing degree on main roof rotation angle.

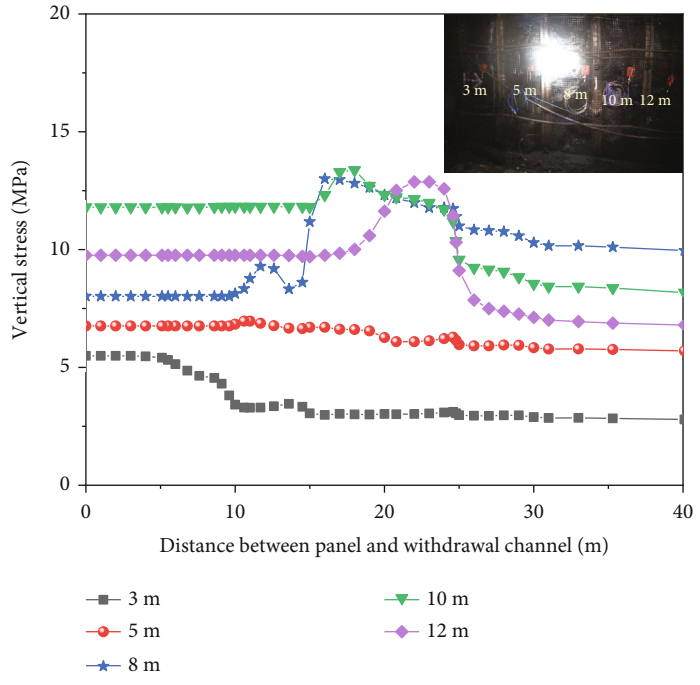


Figure 15: Variation curve of abutment pressure.

It can be seen from Equation (10) that with the increase of the fracture length of main roof, the deflection of main roof increases gradually. In principle, the smaller the fracture length of the main roof is, the smaller the deflection is. However, considering the width of the PWC and the width of the hydraulic powered support in the working face, and the requirements of the site withdrawal operation, the minimum fracture length $d'$ of the main roof can be expressed as

$$d' = X_0 + W + L_k, \tag{11}$$

where the width $X_0$ of plastic zone of coal rib is 7.4 m, the width $W$ of PWC is 4.4 m, and the control distance $L_k$ of

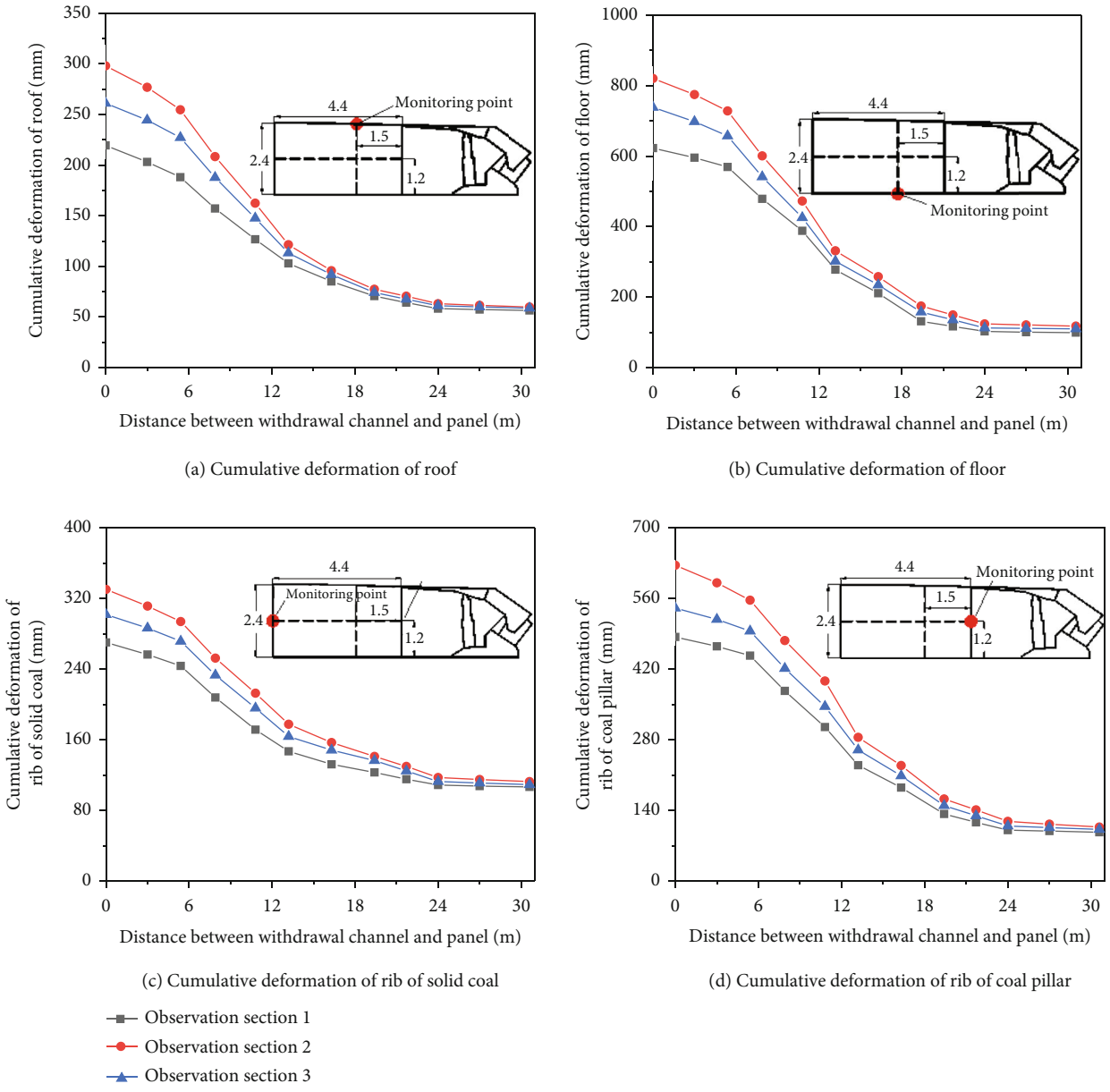


Figure 16: Deformation curve of surrounding rock of PWC.

hydraulic support in working face is 4.8 m, so the minimum fracture length of main roof is 16.6 m.

## 4. Control Effect of Hydraulic Fracturing Pressure Relief on Pre-excavated Withdrawal Channel

*4.1. Control Method Based on Pre-excavated Withdrawal Channel Stability.* According to the above analysis, the surrounding rock deformation of the PWC located in the terminal line of the working face will be affected by the front abutment pressure and the rotary motion of the main roof. Directional fracturing is fundamental to weakening the hard roof in the mine [29, 30]. Therefore, the control method of weakening mining stress and artificial roof cutting by hydraulic fracturing is proposed, as shown in Figure 9.

(1) The fracture network is formed in the roof by hydraulic fracturing, which destroys its integrity, forms the weak structure of key rock strata, and weakens the mechanical properties of the roof, so as to change the stress transfer path and reduce the influence of the front abutment pressure on the PWC

(2) In order to avoid the influence of natural fracture and rotary deformation of the main roof, the main roof is cut off by hydraulic fracturing within the predetermined range above the PWC, so that the PWC

Figure 17: The effect after connection.

is placed below the stable rock beam and the stability of the surrounding rock of the roadway is improved

### 4.2. Numerical Simulation Analysis on Control Effect of Hydraulic Fracturing on Pre-excavated Withdrawal Channel

*4.2.1. Establishment of Numerical Calculation Model.* The numerical calculation model was established by using UDEC to further study the control effect of hydraulic fracturing on the PWC. As shown in Figure 10, the area of hydraulic fracturing is determined by calculating the height of the caving zone and considering the influence range of the front abutment pressure. The target stratum of hydraulic fracturing is the main roof. Weakening the mechanical properties of rock mass by hydraulic fracturing is a process of cracking damage. Therefore, the degree of rock cracking can be expressed by the change of damage variable $D$. According to the parameter calculation formula corresponding to different damage variables [31], the mechanical parameters of sandstone are divided into 6 grades, as shown in Table 2.

*4.2.2. Analysis of Numerical Results.* Figure 11 illustrates the final deformation of the PWC with different damage variables. With the increase of damage variable $D$, the deformation of roof and floor and two ribs gradually decreases; when the damage variable $D$ is 0.3, the variation amplitude of roadway deformation is significantly reduced. At this time, the deformation of roof, floor, rib of solid coal, and rib of coal pillar are 274.3 mm, 783.8 mm, 301.9 mm, and 600.0 mm. Compared with the deformation without fracturing, the deformation decreased by 41.6%, 27.0%, 24.5%, and 20.3%, respectively.

Since the coal pillar has been destroyed when the width is 10 m, the influence of the degree of damage on the stress distribution in the surrounding rock of the roadway when the working face is 15 m away from the PWC is analyzed, as shown in Figure 12. With the increase of the damage variable, the peak stress of the coal pillar, the immediate roof, and the main roof gradually decrease. When the damage variable is 0.3, the variation amplitude of peak stress is significantly reduced. The peak stress of coal pillar decreases from 16.85 MPa to 13.14 MPa, with a decrease of 22.0%. The stress of immediate roof decreased from 14.86 MPa to 11.83 MPa, with a decrease of 20.4%, and the stress of main roof decreased from 10.32 MPa to 9.52 MPa, with a decrease of 7.8%.

The influence of the degree of fracturing on the difference of peak stress is shown in Figure 13. With the increase of damage variable $D$, the difference of peak stress of coal pillar, immediate roof, and main roof increases gradually. This indicates that the greater the degree of rock-cracking damage, the better the weakening effect. When the damage variable $D$ is 0.3, the change of difference decreases obviously, and the difference of coal pillar, immediate roof, and main roof is 3.71 MPa, 3.03 MPa, and 0.80 MPa, respectively.

Figure 14 illustrates the effect of fracturing degree on the rotation angle of main roof. The result shows that the rotation angle of the main roof decreases with the increase of damage variable. When the damage variable $D$ is 0.3, the change of the rotation angle decreases significantly, and the final angle decreases from 2.83° to 1.95°, with a decrease of 31.1%.

Based on the above analysis results, it can be concluded that the stability of the PWC after hydraulic fracturing has been significantly improved. The higher the degree of fracturing, the better the effect of hydraulic fracturing; when the damage variable $D$ is 0.3, the effect is obviously reduced, so the value is determined to be a reasonable degree. It provides a basis for determining parameters of hydraulic fracturing.

## 5. Field Engineering Test

*5.1. Determination of Time-Space Relation of Hydraulic Fracturing.* The pressure relief control of hydraulic fracturing should be coordinated in time and space with the mining of working face. Therefore, hydraulic fracturing should be completed before the PWC is affected by mining. The field measurement results indicate that the influence range of mining is 28 m, and the daily advancing distance of the

working face is 4.8 m. According to the field construction experience, it takes 14 days to drill holes and complete hydraulic fracturing. Therefore, the hydraulic fracturing should be completed 20 days before the working face is connected with the PWC.

According to the principle that the collapsed roof should be filled with gob after hydraulic fracturing, the fracturing height is determined to be 14 m. From the above theoretical analysis, the minimum fracture length of main roof is 16.6 m, and the reasonable position of roof cutting is 9.2 m away from the solid coal rib of the PWC.

*5.2. Analysis of Effect.* The field test was carried out on the PWC of $III32_{upper}1$ working face in Zhuzhuang Coal Mine. In order to evaluate the effect of hydraulic fracturing, a stress observation station was set up in the middle of the PWC, and five horizontal boreholes were drilled in the station. The borehole lengths were 3 m, 5 m, 8 m, 10 m, and 12 m, respectively. And three roadway deformation observation stations were arranged in the PWC: observation section 1 was the upper station (40 m away from the tailgate), observation section 2 was the middle station (95 m away from the tailgate), and observation section 3 was the lower station (130 m away from the tailgate).

The monitoring curve of stress change of station A in the PWC after fracturing is shown in Figure 15. After hydraulic fracturing, the peak value of front abutment pressure is 13.38 MPa, the stress concentration coefficient is 2.39, and the influence range of front abutment pressure is about 22 m. It can be seen from the field measurement results that the peak value of the advanced abutment pressure of the working face is 16.85 MPa, and the influence range of the advanced abutment pressure is about 28 m without fracturing. After fracturing, the peak value of advanced abutment pressure decreased by 20.6%, and the influence range of advanced abutment pressure decreased by 27.3%.

The deformation of the PWC with the advance of the working face is shown in Figure 16. The field observation shows that the deformation of the roadway gradually increases with the advance of the working face. When the working face is about 24 m away from the PWC, the roadway enters the influence range of the advanced abutment pressure of the working face, and the deformation begins to increase significantly. The deformation of the middle station is the largest and the upper station is the smallest. The average deformations of roof, floor, rib of solid coal, and rib of coal pillar of three stations are 259.5 mm, 726.9 mm, 300.8 mm, and 550.3 mm. It can be observed that the locations where deformation occurs after hydraulic fracturing are mainly floor and rib of coal pillar, and the deformation of roof and rib of solid coal is small.

Due to the effective control of the PWC by roof cutting and pressure relief, the surrounding rock is generally stable, the roof does not appear obvious deformation, and the bolt and anchor do not appear fracture and failure, as shown in Figure 17. The withdrawal of the working face adopts the monorail crane withdrawal technology, so the good integrity of the roof is the key to ensure the success of the withdrawal work. The PWC meets the requirements of equipment withdrawal operation, shortens the withdrawal time of working face, ensures the safety of retracement, and achieves significant technical effects.

## 6. Conclusion

(1) Within the influence range of the advanced abutment pressure of the working face, the stress in the interval coal pillar increases significantly with the decrease of the distance from the working face to the PWC. When the width is 10 m, the coal pillar is destroyed. When the working face is 5 m away from the PWC, the deformation speed of the surrounding rock reaches the maximum

(2) The fracture line of the main roof above the PWC is the position where the main roof has the greatest influence on the stability. At this time, the supporting resistance of the hydraulic support increases with the increase of the rotation angle of the main roof, and the deformation of the surrounding rock of the PWC is intensified. The stability of the PWC is maintained by the artificial roof cutting method, and the minimum roof cutting length of the main roof is 16.6 m

(3) It is an effective control method to use hydraulic fracturing technology to release pressure and prevent the main roof fracturing above the PWC. Furthermore, the higher the degree of fracturing, the better the control effect. Finally, the reasonable degree is determined as the damage variable is 0.3

(4) The time-space relationship of hydraulic fracturing is determined according to the field conditions. Moreover, the measurement results indicate that the mining stress is obviously reduced and the deformation of the PWC is effectively controlled by the hydraulic fracturing

## Data Availability

The data used to support the findings of this study are included within the article.

## Conflicts of Interest

The authors declare that they have no conflicts of interest.

## Acknowledgments

The work was supported by the National Natural Science Foundation of China (No. 52074267). The authors gratefully acknowledge the financial support of the agency mentioned above.

## References


[1] D. Wichlacz, T. Britten, and B. Beamish, "Development of a pre-driven recovery evaluation program for longwall operations," in *2009 Coal operators' conference*, pp. 23–36, University of Wollongong, New South Wales, 2009.

[2] D. C. Oyler, R. C. Frith, D. R. Dolinar, and C. Mark, "International experience with longwall mining into pre-driven rooms," *Proceedings 17th International Conference on Ground in Mining*, , pp. 44–53, West Virginia University, Morgantown, 1998.

[3] J. Emery, I. Canbulat, and C. Zhang, "Fundamentals of modern ground control management in Australian underground coal mines," *International Journal of Mining Science and Technology*, vol. 30, no. 5, pp. 573–582, 2020.

[4] C. Zhu, Y. Yuan, Z. Chen, Z. Liu, and C. Yuan, "Study of the stability control of the rock surrounding double-key strata recovery roadways in shallow seams," *Advances in Civil Engineering*, vol. 2019, Article ID 9801637, 21 pages, 2019.

[5] J. Listak and E. Bauer, "Front abutment effects on supplemental supports in pre-driven longwall equipment recovery rooms," in *The 30th U.S. Symposium on Rock Mechanics*, pp. 19–22, OnePetro, 1989.

[6] B. Wang, F. Dang, S. Gu, R. Huang, Y. Miao, and W. Chao, "Method for determining the width of protective coal pillar in the pre-driven longwall recovery room considering main roof failure form," *International Journal of Rock Mechanics and Mining Sciences*, vol. 130, p. 104340, 2020.

[7] F. T. Wang, D. L. Shao, T. C. Niu, and F. J. Dou, "Progressive loading characteristics and accumulated damage mechanisms of shallow-buried coal pillars in withdrawal roadways with high-strength mining effect," *Chinese Journal of Rock Mechanics and Engineering*, vol. 41, no. 6, pp. 1148–1159, 2022.

[8] H. W. Lv, "The mechanism of stability of pre-driven rooms and the practical techniques," *Journal of China Coal Society*, vol. 39, no. S1, pp. 50–56, 2014.

[9] H. E. Yanjun, S. O. Yaxin, S. H. Zhanshan, L. I. Junqi, C. H. Kai, and L. I. Zhiping, "Study on failure mechanism of withdrawal channel's surrounding rock during last mining period," *China Safety Science Journal*, vol. 32, no. 2, pp. 158–166, 2022.

[10] Y. J. He and J. Li, "Stress distribution and optimum spacing determination of double-withdrawal-channel surrounding rocks: a case study of chinese coal mine," *Shock and Vibration*, vol. 2021, Article ID 9973634, 16 pages, 2021.

[11] S. C. Gu, B. N. Wang, R. B. Huang, and Y. Miao, "Method for determining the load on and width of coal pillar at the recovery room end of fully mechanized longwall mining," *Journal of China University of Mining and Technology*, vol. 44, no. 6, pp. 990–995, 2015.

[12] G. U. Shuancheng, H. U. Rongbin, L. I. Jinhua, and S. U. Peili, "Stability analysis of un-mined coal pillars during the pressure adjustment prior to working face transfixion," *Journal of Mining and Safety Engineering*, vol. 34, no. 1, pp. 60–66, 2017.

[13] F. Liu and J. Zhongxi, "Research on deformation mechanism of retracement channel during fully mechanized caving mining in superhigh seam," *Advances in Civil Engineering*, vol. 2018, Article ID 1368965, 13 pages, 2018.

[14] K. Lv, F. He, L. Li, X. Xu, and B. Qin, "Field and simulation study of the rational retracement channel position and control strategy in close-distance coal seams," *Energy Science and Engineering*, vol. 10, no. 7, pp. 2317–2332, 2022.

[15] B. Wang, F. Dang, W. Chao, Y. Miao, J. Li, and F. Chen, "Surrounding rock deformation and stress evolution in pre-driven longwall recovery rooms at the end of mining stage," *International Journal of Coal Science and Technology*, vol. 6, no. 4, pp. 536–546, 2019.

[16] C. Li, X. Guo, X. Lian, and N. Ma, "Failure analysis of a pre-excavation double equipment withdrawal channel and its control techniques," *Energies*, vol. 13, no. 23, p. 6368, 2020.

[17] G. R. Feng, G. Wang, and P. Wang, "Study on rational width of the end-mining coal pillar of extra-thick mining working face in permo-carboniferous igneous rock intrusion area," *Journal of Mining and Safety Engineering*, vol. 36, no. 1, pp. 87–94, 2019.

[18] M. Xingen, H. Manchao, W. Yajun, Z. Yong, Z. Jiabin, and L. Yuxing, "Study and application of roof cutting pressure releasing technology in retracement channel roof of Halagou 12201 working face," *Mathematical Problems in Engineering*, vol. 2018, Article ID 6568983, 15 pages, 2018.

[19] Y. F. Guo and Y. Hong, "Research and application of roof cutting and pressure release technology of retracement roadway in large height mining working face," *Geotechnical and Geological Engineering*, vol. 39, no. 2, pp. 1289–1298, 2021.

[20] F. He, K. Lv, X. Li, B. Qin, and L. Li, "Failure mechanism and control of lower retracement channel in close-distance double-thick coal seams," *Shock and Vibration*, vol. 2021, Article ID 6651099, 19 pages, 2021.

[21] F. Zhang, X. Wang, J. Bai, W. Wu, B. Wu, and G. Wang, "Fixed-length roof cutting with vertical hydraulic fracture based on the stress shadow effect: a case study," *International Journal of Mining Science and Technology*, vol. 32, no. 2, pp. 295–308, 2022.

[22] B. Qin, F. He, X. Zhang et al., "Stability and control of retracement channels in thin seam working faces with soft roof," *Shock and Vibration*, vol. 2021, Article ID 8667471, 12 pages, 2021.

[23] Z. Wang, J. Li, and B. Qin, "Study on stability and control of retracement channel with thin bedrock and broken roof," *Safety in Coal Mines*, vol. 52, no. 6, pp. 230–236, 2021.

[24] H. Kang, H. Lv, X. Zhang, F. Gao, Z. Wu, and Z. Wang, "Evaluation of the ground response of a pre-driven longwall recovery room supported by concrete cribs," *Rock Mechanics and Rock Engineering*, vol. 49, no. 3, pp. 1025–1040, 2016.

[25] X. B. Feng and S. Wu, "Surrounding rock control of the retreat passage of the fully mechanized caving face under the thick coal seam," *Coal Science and Technology*, vol. S2, pp. 77–83, 2021.

[26] J. Y. Yang and L. Zhu, "Characteristics of overlying strata movement and control technology of final mining section in fully mechanized mining face with double retracting passage," *Safety in Coal Mines*, vol. 52, no. 12, pp. 240–246, 2021.

[27] Z. Zhang, M. Deng, J. Bai, S. Yan, and X. Yu, "Stability control of gob-side entry retained under the gob with close distance coal seams," *International Journal of Mining Science and Technology*, vol. 31, no. 3, pp. 321–332, 2020.

[28] M. Wang, E. L. Xia, W. L. Shen, X. X. Liu, D. J. Zheng, and X. Liu, "Determining method of the driving time for the gob-side entry considering the effect of gangue compression," *Journal of Mining & Safety Engineering*, vol. 37, no. 5, pp. 928–935, 2022.

[29] Y. Xing, B. Huang, B. Li et al., "Investigations on the directional propagation of hydraulic fracture in hard roof of mine:

utilizing a set of fractures and the stress disturbance of hydraulic fracture," *Lithosphere*, vol. 2021, article 4328008, 20 pages, 2021.

[30] Q. Chang, X. Yao, X. Wang, S. Yang, Y. Sun, and H. Liu, "Investigation on hydraulic fracturing and cutting roof pressure relief technology for underground mines: a case study," *Lithosphere*, vol. 2021, article 4277645, 15 pages, 2021.

[31] J. W. Liu, *Research on Mechanism and Control of Stress Field Change of Artificial Cracking Coal and Rock Mass*, China University of Mining and Technology, 2020.